

Influence of polymer molecular weight on the solid-state structure of PEG/monoolein mixtures

Denny Mahlin^{a,*}, Johan Unga^b, Annika Ridell^a, Göran Frenning^a, Sven Engström^b

^a Department of Pharmacy, Uppsala Biomedical Centre, Uppsala University, Box 580, SE-751 23 Uppsala, Sweden

^b Department of Chemical and Biological Engineering, Chalmers University of Technology, SE-412 96 Göteborg, Sweden

Received 27 May 2005; received in revised form 17 October 2005; accepted 20 October 2005

Available online 10 November 2005

Abstract

The polar lipid monoolein (MO) and poly(ethylene glycol), PEG, of different molar mass (1500, 4000 and 8000) were melted, mixed and left to solidify at room temperature. Analysis of the solid mixtures by differential scanning calorimetry (DSC) and small angle X-ray scattering (SAXS) revealed that a phase separation occurs when MO is present in sufficient amounts. The molecular weight of the polymer determines the amount of MO that has to be added before a separate MO phase can be detected. To further understand this behaviour, the folding of the polymers and the thickness of the amorphous domains within the lamellar structure of PEG were determined by calculation of the one-dimensional correlation function from the experimental SAXS data. It revealed that the presence of MO makes the crystalline domains of PEG 1500, which crystallizes unfolded, increase at the expense of the amorphous domains. PEG 4000 and PEG 8000 obtain a higher degree of folding when the MO content in the mixtures increases. Furthermore, a second form of MO was detected when it phase separated from PEG 1500 and 4000. This behaviour was argued to be due to the secondary crystallization of the PEGs.

© 2005 Elsevier Ltd. All rights reserved.

Keywords: Crystallization; Phase formation; Lipid–polymer mixture

1. Introduction

Lipid-based drug formulations have the potential to serve as carriers both for poorly soluble drugs and compounds sensitive to enzymatic and chemical degradation. Therefore, there has been a considerable amount of scientific interest in these type of systems for delivery of lipophilic drugs and peptides [1–4]. The properties of the lipid as a drug carrier can in many cases be improved by formation of dispersions, e.g. solid lipid nanoparticles (SLN) [5], emulsions [6] or microemulsions [7].

Solid dosage forms are generally preferred to liquid ones, primarily owing to their better storage stability. Combining the benefits of dispersed lipid with the properties of formulations in the solid-state is, therefore, an attractive prospect. Several methods of producing such systems have been presented. The ‘dry emulsion’ method, where the liquid is removed from an emulsion by spray drying [6] or lyophilization [8] is the most common concept. These drying techniques have been used to

remove the water from SLN dispersions [9] and spray-drying has been applied to dry a liquid dispersion of a cubic phase [10]. Common for all these systems is that the liquid dispersion reconstitutes when they are added to water.

In a recent study, another type of solid lipid system was characterized: a solid mixture of the polar lipid monoolein (1-glyceryl monooleate, MO) and poly(ethylene glycol) (PEG) of average molecular weight 4000 g/mol (PEG 4000) [11,12]. The idea was to create a pre-dispersed lipid system similar to a dry emulsion. It was found that MO and PEG 4000 phase separate when the mixture contains more than 5 wt% MO. In addition, MO induced a partial stabilization of the folded form of PEG 4000 and was partially intercalated into its amorphous lamellae.

Monoolein, a polar lipid formed during digestion of triglycerides, is non-toxic and has been approved for pharmaceutical use. It has been utilized in many areas, such as drug delivery [13–15] and protein crystallization [16].

PEG is a hydrophilic straight chain polymer available in a large number of molecular weights. Those of average molecular weights over ~ 1000 g/mol are solid at room temperature. PEG in the solid-state is semi-crystalline and forms a lamellar structure. The degree of folding is determined by the chain length. The primary crystallization, where crystals

* Corresponding author. Tel.: +46 18 471 4372; fax: +46 18 471 4377.

E-mail address: denny.mahlin@farmaci.uu.se (D. Mahlin).

of higher chain folding are commonly formed, is followed by a gradual extension of the polymer chains to more stable conformations [17]. Solid (PEGs) are common carriers in drug dispersions, one example being the dispersion of the drug griseofulvin in PEG 6000 [18,19].

In the present study, we have expanded the scope and examined solid-state mixtures of MO and PEGs of lower (PEG 1500) and higher (PEG 8000) molecular weights, as well as the intermediate PEG 4000. The solid mixtures were prepared by co-melting and were characterized using differential scanning calorimetry (DSC) and small angle X-ray scattering (SAXS).

The effect of additives in solid PEGs and other semi-crystalline polymers has recently been investigated in different contexts. Solid-state mixtures of PEG and various surfactants have been studied [19–21] as has the melting of mixtures of PEGs and fatty acids [22]. Several studies have examined the solid-state structure of semi-crystalline polymers, including the influence of an added second component [23–26]. However, to our knowledge, no such structure analysis of semi-crystalline polymers when mixed with a lipid component has been performed.

2. Experimental

2.1. Materials

PEG 1500 (mol wt. 1400–1600, Merck, Germany), PEG 4000 (mol wt. 3500–4500, Merck, Germany) and PEG 8000 (mol wt. 7000–9000, Sigma, Germany) were used as received. MO of technical grade (RYLO MG 19 Pharma, lot no. 2119/83) was a gift from Danisco Cultor (Denmark).

2.2. Sample preparation

Monoolein and PEG were weighed and mixed in 3 ml glass ampoules at 120 °C for 20 min while subjected to intermittent vortexing. The total sample weight was 500 mg for all samples. All samples solidified within 1 day at room temperature and were stored at room temperature for at least 6 weeks before DSC and SAXS measurements were conducted. Fewer samples of PEG 4000 were prepared than of the other PEGs since the MO/PEG 4000 system had been investigated in previous work [11]. The samples (3, 8 and 25 wt% MO) included here were used for validation of the preparation method. In addition, a physical mixture of pure PEG 8000 and MO was prepared to be used for validation of the peak-subtraction procedure (Section 2.4).

2.3. DSC

DSC was performed in an N₂-atmosphere using a Seiko DSC 220 differential scanning calorimeter (SSC/5200H, Seiko, Japan). The analysis of each sample (2–4 mg) was started after 5 min at 0 °C; the samples were heated at a rate of 5 °C/min until a temperature of 150 °C was attained, at which temperature the sample had completely melted. Each type of sample was run 1–3 times. The heat of fusion per gram sample

(ΔH_m) was determined by measuring the melting peak area for each component. The weight fraction of the MO phase was calculated as

$$X_{\text{MO phase}} = \frac{\Delta H_m^{\text{MO, sample}}}{\Delta H_m^{\text{MO, pure}}}$$

2.4. SAXS

SAXS experiments were performed on a Kratky camera (Hecus X-ray systems, Graz, Austria) with a linear position-sensitive detector (MBraun, Garching, Germany) using Cu K_α X-rays (wavelength 1.542 Å) provided by an X-ray generator (Philips, PW 1830/40, The Netherlands) operated at 50 kV and 40 mA. A tungsten beam stop was used. The samples were placed between mica windows and the temperature was controlled by a Peltier element to 20 °C. Each measurement was performed for 3 h in a vacuum.

From the experimental SAXS diffractograms ($0.02 \text{ \AA}^{-1} < q < 0.65 \text{ \AA}^{-1}$), the one-dimensional correlation function, $\gamma_1(x)$, the long period, L , the crystalline layer thickness, l_c , and the amorphous layer thickness, l_a , were calculated according to the procedure described previously [11,12], but with the following modifications: firstly, different measures were taken to reduce the effects of the peak resulting from the pure MO phase because of its overlap with the peaks of interest for the one-dimensional correlation function. A theoretical peak shape superimposed on a polynomial background was fitted to the experimental diffraction intensity in the region of the peak (the exact location depended on the shape of the diffractogram, but the fit was typically made for q -values between 0.08 and 0.2 \AA^{-1}). A peak of the split Pearson VII type and a cubic background were used. The expression for the split Pearson VII peak reads [27]

$$I(q) = \begin{cases} H \left[1 + \left(\frac{1+A}{A} \right)^2 \times (2^{1/R_L} - 1) \times \left(\frac{q-T}{W} \right)^2 \right]^{-R_L} & ; q \leq T \\ H \left[1 + (1+A)^2 \times (2^{1/R_H} - 1) \times \left(\frac{q-T}{W} \right)^2 \right]^{-R_H} & ; q > T \end{cases}$$

where T is the position of the peak maximum, H the peak height, W the full width at half maximum, A the asymmetry parameter, R_L the decay rate for $q < T$, and R_H the decay rate for $q > T$. This peak shape is rather general and interpolates between peaks with Lorentzian tails (obtained for R_L or $R_H = 1$) and peaks with Gaussian tails (obtained in the limit R_L or $R_H \rightarrow \infty$). Once a satisfactory fit had been obtained, the peak contribution to the observed intensity was calculated and subtracted from the experimental diffraction intensity. A polynomial interpolation was used for q -values close to the peak maximum, where the peak-corrected intensity exhibited errors resulting from the subtraction of two large numbers.

Secondly, because the locations of peaks differed from one sample to the other, it was necessary to use somewhat different regions for fitting the Porod–Ruland and the Debye–Bueche

expressions to the experimental data. As in our previous work, these expressions were used to extrapolate the experimental intensity to $q=0$ and $q=\infty$. The Porod–Ruland expression was typically fitted to the data for $q > 0.11 \text{ \AA}^{-1}$ and the Debye–Bueche expression for $q < 0.034 \text{ \AA}^{-1}$.

3. Results and discussion

3.1. DSC

DSC was performed on solidified samples of co-melted PEG and MO. The PEG and the MO phase-separated upon solidification as was evident from the presence of two separate melting peaks in the DSC melting thermogram (Fig. 1). These peaks essentially overlapped the melting points of pure MO and PEG, indicating that the phases formed were relatively pure in either component. However, the shape of the melting peaks changed over time during the first weeks after preparation. The general tendency for the peak that was associated with the melting of PEG was that a freshly prepared sample displayed a double peak, which slowly transformed into a single melting event over time. In Fig. 2 typical thermograms of mixtures before and after storage are shown. However, this transformation was not obvious in PEG 1500 which displayed one stable peak shortly after sample preparation. The folded

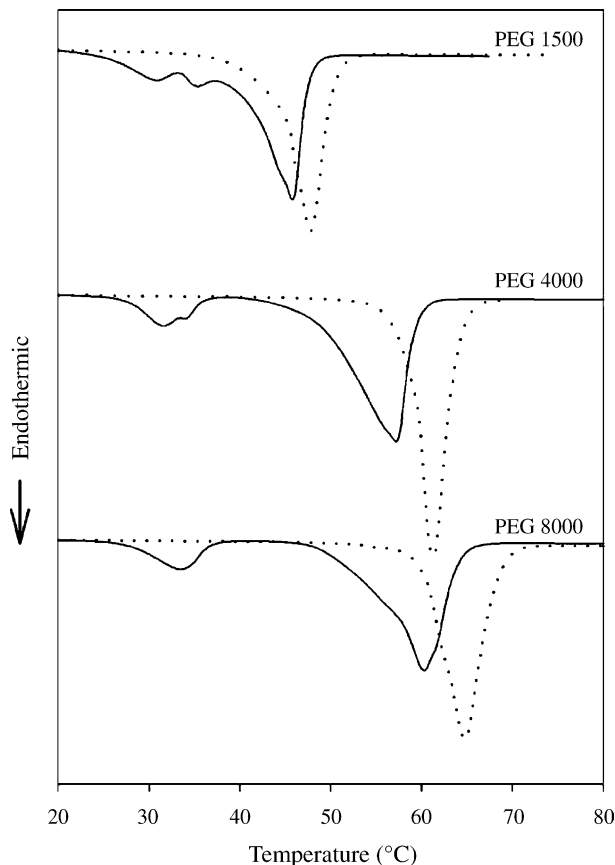


Fig. 1. Typical DSC thermograms for the three different molecular weights of PEG with 25% MO added, displaying the melting peaks of the MO and PEG phases. The dotted lines are the thermograms of the pure PEGs. All data is normalized by the weight of PEG in the samples.

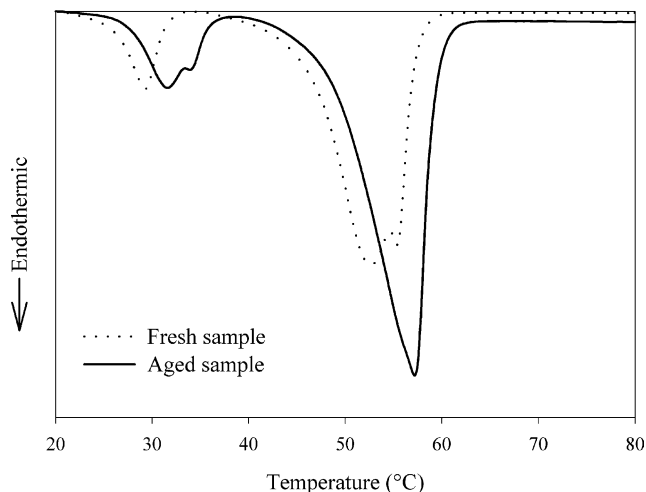


Fig. 2. DSC thermograms of a freshly prepared mixture of PEG 4000 with 25% MO (dotted line) and the same mixture after storage for 6 weeks (solid line).

form in this case must have, if present at all, very quickly transformed into the unfolded one. The melting temperature of MO increased over time and, for some samples that contained higher amounts MO (as described in detail below), double melting peaks, more or less overlapping, appeared after a few weeks of storage. When samples contained lower amounts of MO no melting peak of MO could be detected on freshly prepared samples. However, a single melting peak appeared in these samples upon storage. Because of this, the samples were stored for at least 6 weeks before analysis. After that time, no further change in melting behaviour could be observed in the thermograms. The melting peaks after 6 weeks were still quite broad, in particular for PEG which may have been a consequence of the PEG being polydisperse. However, the important reason for the broadness of these peaks is the different degrees of folding that PEG can adopt, as discussed in more detail below.

The melting temperature corresponding to the MO phase was almost constant for all compositions (0–100% MO, data not shown). In contrast, the PEG melting point decreased gradually as the amount of MO in the sample as a whole increased. This is indicative of a monotectic phase behaviour [28] meaning that the components do not mix in the solid-state. The reason for melting point depression of PEG is that it melts in the presence of liquid MO.

The amount of MO phase that had formed at different total compositions was calculated from DSC melting enthalpy data. It can be seen in the diagram in Fig. 3, where the amount of MO phase per gram sample is plotted as a function of the total weight fraction of MO (X_{MO}), that the amount of MO phase formed depended on the molecular weight of the PEG present in the mixture. The samples containing PEG 4000 were identical with the results obtained in our previous work [11]; to facilitate the comparison with the other molecular weights, the old data are included in the diagram. The general appearance of the different plots in the diagram was compliant with the previously described MO/PEG 4000 system. At low wt% MO, no or very low amount of MO phase was formed and the

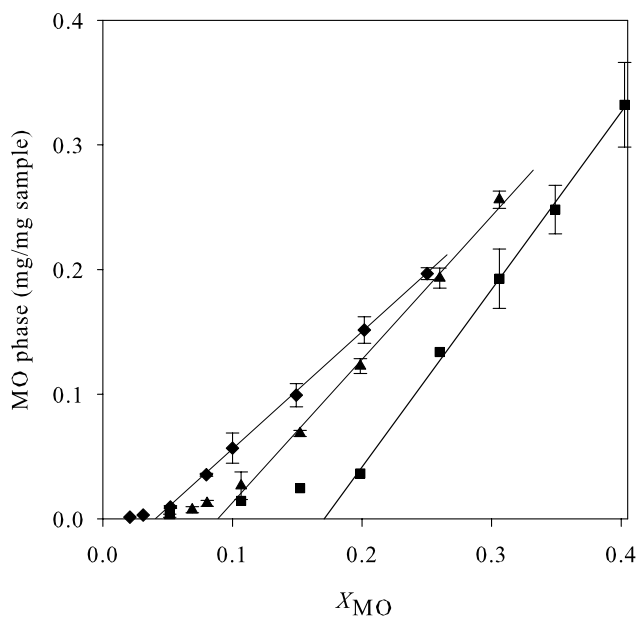


Fig. 3. Amount of MO phase per gram of sample calculated from DSC melting enthalpy data as a function of the total amount of MO in the samples. The PEG molecular weights used in the MO/PEG systems were 8000 (diamonds), 4000 (triangles) and 1500 (squares). Error bars indicate standard deviations.

increase in the MO phase with the increasing proportion of MO was modest. At a higher total MO content the plot became linear with a slope closer to one.

This means that the PEG phase at a higher MO content can be considered to be saturated with MO. Increasing the total MO content above the saturation point will not result in more MO intercalation into the PEG, but rather, all additional MO will add to the separate MO phase. The plot of MO/PEG 8000, for instance, exhibited a linear region starting at 5 wt% MO. This starting point of the linear part of the curve was shifted to a higher total MO content as the molecular weight of the PEG was decreased. For PEG 1500 and PEG 4000 there was an MO phase present before the onset of the linear region, slowly increasing with increasing total amount MO, whereas for PEG 8000, virtually no MO could be detected by DSC before the linear region appeared.

Under the assumption that all MO that could not be detected within the separate MO phase was incorporated into the PEG-rich phase, the DSC-data shows that the PEG-rich phase of PEG 1500 contained approximately 16 wt% MO, PEG 4000 8.5 wt% and PEG 8000 5 wt% MO at saturation. Another difference between the different polymer molecular weights was observed in the DSC thermograms (Fig. 1): MO displayed a double melting peak when mixed with PEG 4000 in higher proportions (15–25%). In the case of PEG 1500 these two phases were even more apparent, with the peaks being fairly well separated and detectable for the samples containing 20–40% MO. The appearance of the second peak coincides with the start of the linear region in Fig. 3, indicating that the MO phase with the lower melting point was primarily formed after the PEG had been saturated with MO. For PEG 8000 there

was only one single MO peak detectable in the thermogram for all compositions.

The extent of the folding of the PEG crystals can be determined to some degree from the shape of the melting peak since a folded polymer has a lower melting- or refolding point than more extended ones [20]. It is well established that the various PEGs are stable in differently folded forms depending on their molecular weight, the preparation method and the time they have been stored [17]. In the present study the peaks were not very well separated, which made it difficult to draw conclusions from DSC data only.

3.2. SAXS

The SAXS technique provides an alternative way of studying the folding of semi-crystalline polymers and was, therefore, used in this study. The peaks present in the SAXS diffractograms (Fig. 4) originated from the lamellar packing of both MO and PEG. A MO peak could be found at a constant q ($\approx 0.13 \text{ \AA}^{-1}$), while the shape and position of the PEG peaks varied with the molecular weight of the PEG and the sample composition.

In this study, the method used for the SAXS data analysis was modified from that used in a previous work by us (Section 2). The reason for this was that truncating the experimental diffractogram (at $q \approx 0.09 \text{ \AA}^{-1}$) to eliminate the MO peak did not produce results of sufficiently high quality, especially for the MO/PEG 1500 system, for which, in some cases, the second-order lamellar peak of the PEG and the MO-phase peak were partially overlapping. The fit of a Split-Pearson VII-function to the peak originating from the added lipid was good (Fig. 5). The ensuing subtraction of the peak enabled a larger region of q -values to be used when calculating the correlation function of the polymer packing. Plots of representative correlation functions are shown in Fig. 6. Application of this modified analysis method to the old SAXS data yielded results that were

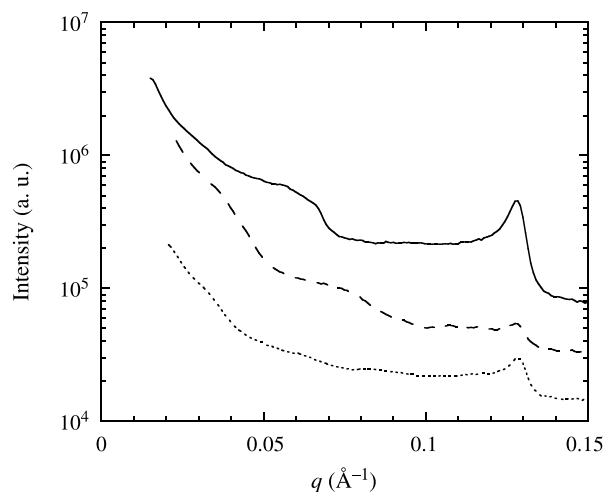


Fig. 4. Typical diffraction patterns for mixtures of MO and PEGs of different molecular weights: PEG 1500 (solid lines), PEG 4000 (dashed lines), and PEG 8000 (dotted lines). The MO contents of the mixtures are 10% (PEG 1500) and 8% (PEG 4000 and 8000).

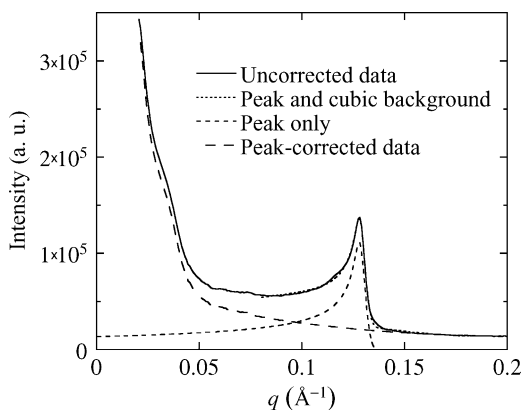


Fig. 5. Result of the peak-correction procedure, here illustrated for the 75% PEG 8000/25% MO sample.

comparable to those presented in our previous article. However, it should be noted that the values were generally 10% lower than those obtained with the old approach. To validate the peak subtraction method a physical mixture of PEG 8000 and MO was prepared and analysed. The resulting correlation functions for pure PEG 8000 and the physical mixture after subtraction of the MO diffraction peak are shown in Fig. 7. Even though the shape of the correlation function seems to be somewhat affected by the peak subtraction, the position of the first maximum was essentially unaltered (it decreased by <1%). Moreover, the value of l_a , calculated from the minimum value and the location of the first maximum of γ_1 , was also essentially unaffected for a MO content of 10% (<1% increase). When the MO content in the physical mixture was 20%, l_a increased by approximately 7% compared to the value obtained for the pure PEG 8000. Apparently, the values obtained for the long period are virtually unaffected by the peak subtraction, whereas the values obtained for the amorphous and crystalline domains change somewhat when the MO content exceeds 10%.

Samples with 100% PEG 4000 did not show any peaks in the diffraction spectra as had been reported earlier, indicative of highly crystalline packing of unfolded PEG molecules [11]. In Fig. 8, the long periods, L , and the crystalline and amorphous layer thickness, l_c and l_a , are shown as a function of X_{MO} .

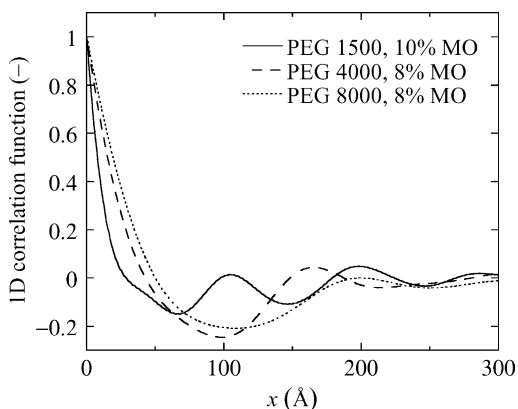


Fig. 6. One-dimensional correlation functions calculated for PEG/MO mixtures with the compositions indicated in the figure.

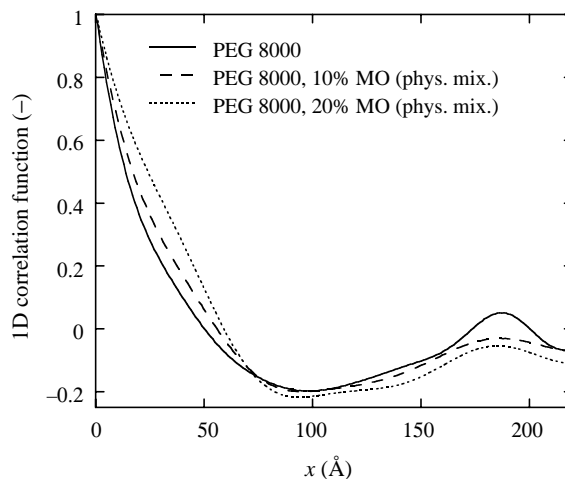


Fig. 7. One-dimensional correlation functions calculated for pure PEG 8000 and the physical mixture of PEG 8000 with 10 and 20% MO.

For samples with PEG 8000 alone repetitive peaks appeared in the diffractogram with a long period, L , of approximately 187 Å. When processing the data in the same way as done by Santa Cruz [29] the crystalline part of the lamellar stacks, l_c , was found to be 157 Å. This value corresponds well with the distance for twice-folded PEG 8000 [17]. One should, however, be aware that the first reflections for unfolded or once-folded PEG 8000 cannot be detected by our equipment because the q -values were too low (below 0.03 \AA^{-1}).

When adding MO to the PEG 8000, a similar qualitative process was seen as was reported for the MO/PEG 4000 system [11]. However, the shorter amorphous part of the lamellar stacks, l_a , was constant at about 40 Å at a MO content of 5 wt% or more. The long period, and thus l_c , of the lamellar stacks stayed constant up to 15 wt% whereupon both L and l_c decreased markedly. This decrease probably indicates a higher proportion of three-times folded PEG. The interpretation of the results for PEG 8000 at high MO content is complicated by the fact that the possible number of folds that the polymer chain can attain may be up to at least three. Nevertheless, we find it fair to say that this data supports that MO stabilizes the more folded forms of PEG 8000 in a similar manner as found for PEG 4000.

PEG 1500 on the other hand displayed a different folding pattern. For pure PEG 1500 l_a was 20 Å which was similar to the value obtained for other PEGs. As no MO is present, the amorphous domains should, consequently, consist mostly of disordered chain ends. As MO was added this value decreased to approximately 15 Å where it stayed constant through all compositions. In contrast, the length of the crystalline domain increased drastically until it was comparable to the length of the fully extended PEG 1500 helix. This increase in l_c suggests that the helices become fully extended and the polymer chain ends more ordered, and hence a part of the crystalline domain, at the expense of the amorphous domain. Incorporation of MO in the amorphous domain can explain that l_a does not become zero as the l_c attains the value of a fully extended and crystalline PEG 1500 helix.

It might seem contradictory that for PEG 1500 l_c increases when MO is added while it decreases for PEG 4000 and PEG 8000. That is not necessarily the case. According to our observations both by DSC and SAXS PEG 1500 crystallizes into an unfolded conformation whereas the higher molecular weight PEGs become folded. This means that in PEG 1500 only chain ends are involved in the amorphous regions whereas in the longer PEGs both ends and folds constitute the amorphous parts. The secondary crystallization process will hence be quite different in the two cases. MO seems to promote ordering of the PEG chain ends, as in PEG 1500, but chain folds are intrinsically prevented from becoming crystalline. In PEG 4000 and PEG 8000 where such folds are present the amorphous phase will prevail even when MO is added. Therefore, it seems reasonable that a change in the properties

of the amorphous phase, caused by the incorporation of MO, may have quite different effects on the different systems.

3.3. Intercalation and crystallization of MO

For PEG 4000 it has been shown by wide-angle X-ray diffraction that the crystal structure is preserved upon addition of MO [11]. It is likely that this is equally true for PEG 8000 and PEG 1500 since they crystallize in the same crystal form, and as, from the DSC, it can be seen that there are only minor shifts in melting point in the presence of MO. This leads to the conclusion that essentially no MO was intercalated into the crystalline parts of the PEGs. Hence, it can be concluded that the MO not detected as a separate MO phase by DSC is intercalated into the amorphous domains of the lamellar stacks. However, there is also a chance that it can end up outside the lamellar stacks or possibly cover the surfaces of crystallites of PEG. It seems unlikely that MO domains outside the lamellar stacks would not crystallize and then be detected by DSC, but the surface coverage of crystallites cannot be excluded.

In the MO/PEG 1500 and MO/PEG 4000 mixtures, two different MO phases could be detected using DSC. However, in the SAXS diffractogram there was only one peak visible associated with the MO packing. The melting points overlap those of the β - and the β' -polymorphs of MO [30], but since SAXS cannot discriminate between the two forms it is unclear if both these are present. Hence, it cannot be excluded that the double melting peak is caused by a difference in the incorporation of the MO domains in the PEG structure of the same type of polymorph. WAXS has earlier indicated that the β -form is present at higher wt% of MO [11].

By qualitatively analyzing the shape of the PEG melting peaks in the DSC thermograms obtained from different samples during the first weeks of storage, it was apparent that the relative amount of the folded forms decreased upon storage. This was concluded from observations of the overlapping melting peaks of PEG, where the peak area of the lower melting point decreased while the area corresponding to the higher one increased over time. This is consistent with the idea that polymer chains unfold during secondary crystallization [31]. As this unfolding of PEG occurred in parallel with the appearance of the second MO phase, it is likely that this was formed by expulsion of MO from the PEG structure and that this arose as a consequence of the secondary crystallization. This may also explain the differences in the amounts of MO incorporated in the PEG lamellae. For PEG 1500, which incorporates the highest amount of MO, the secondary crystallization is very fast. The longer PEGs clearly had a distinguishable primary and secondary crystallization.

On the basis of these observations, we hypothesize that the phase formation in a MO/PEG mixture comes about in the following way: at early stage solidification, phase separation produces a pure MO phase, and a PEG-rich phase that incorporates a certain amount of MO. Upon storage, further crystallization occurs, i.e. a secondary crystallization during which the chains of the folded polymers may unfold and

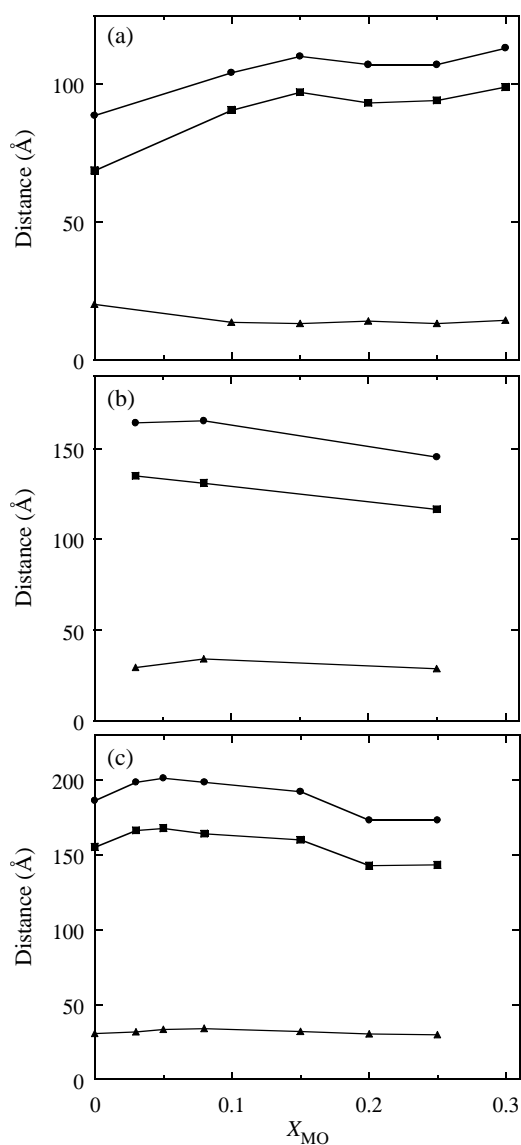


Fig. 8. Results obtained from analysis of SAXS data for mixtures of MO and PEGs of different molecular weights: (a) PEG 1500, (b) PEG 4000, and (c) PEG 8000. Circles indicate the long period (L), squares the crystalline layer thickness (l_c), and triangles the amorphous layer thickness (l_a).

crystallization at the crystalline–amorphous interface occurs, leading to extension of the crystalline domains for all PEGs. The secondary crystallization causes expulsion of MO from the PEG-rich phase whereby a second MO phase forms. Hence, there are two forms of separate MO phase; the one that is formed at the early stage solidification and the phase formed during secondary crystallization of the PEG-rich phase. It is likely that those two forms form quite different domains in the samples. The ones formed at solidification of the samples are probably clearly separate from the PEG-rich phase. The one formed during storage by expulsion from the PEG-rich phase is likely somehow confined within the PEG structure forming smaller aggregates due to the rigid environment. This difference could also explain their difference in melting points. In DSC measurements performed on freshly prepared samples virtually no MO phase could be detected below the point of onset of the linear region of the MO-phase/amount MO curve in Fig. 3. After storage MO melting could also be detected at lower total MO amounts. This is consistent with the idea of two different mechanisms of MO phase formation. The explanation behind the absence of a second MO phase in mixtures with PEG 8000 is that less MO remains in the PEG-rich phase upon phase separation at an early stage of solidification and that PEG 8000 has a lower tendency to unfold during secondary crystallization, whereby less MO will be expelled from the lamellar structure. For PEG 1500 on the other hand, a large amount of MO is trapped in the PEG rich phase and will eventually form the second MO phase or be intercalated into the amorphous domains of the lamellar structure.

The mechanism behind the early stage phase separation is not known for this system. The theory of liquid–liquid phase separation tells us that in the normal case a polymer of high molecular weight has a stronger driving force for separation than the same polymer with a lower molecular weight [32]. This could explain why PEG 8000 incorporates less MO during early stage solidification, when the system still is quite liquid like.

Whether the samples at the time for measurement had reached equilibrium or were in meta-stable state cannot be concluded from our data but the latter seems more likely. A reasonable assumption is that MO has an equilibrium solubility in the PEG-rich phase of a certain PEG at a specific temperature that is independent of the composition of the sample. That would result in a phase behaviour where no MO phase would exist until the PEG had been saturated with MO and once saturation was achieved, the amount of MO phase would increase linearly when more MO was added. Our samples do not show that appearance (Fig. 3), which supports the idea of a meta-stable state. Hence, the solid-state structure formed is evidently determined by a balance between kinetic and thermodynamic properties of the system.

4. Summary and conclusions

In a previous publication, the formation of separate phases in solid mixtures of MO and PEG 4000 has been studied [11]. In order to find an explanation for the mixing behaviour,

we have here expanded the investigation to include PEGs of different molecular weight (1500, 4000 and 8000). The results revealed that a lower molecular weight PEG is able to intercalate more MO into its structure than PEGs of higher molecular weight. PEG 1500 crystallizes with fully extended helices when MO is present in proportions higher than 15 wt%. It is most likely that the amorphous volume of the lamellar structure consists of intercalated MO. In PEG 4000 and PEG 8000, in contrast, the degree of folding increases as the amount of MO in the samples increases, making the volume of the amorphous domains large enough to accommodate the amount of MO intercalated in these mixtures.

Increasing the amount of MO decreases the melting point of all three PEGs. A higher degree of folding could have been an explanation for this, unless it was evident, as revealed by SAXS, that the crystallinity increased in PEG 1500 upon MO addition. This reinforces the assumption that the presence of molten MO is the main reason for the melting point decrease and that the system has a monotectic phase behaviour.

Preparation of samples in which the wt% of MO in the mixtures exceeded the concentration where the PEG-rich phase was saturated resulted in the formation of two separate MO phases. Both forms of MO phase were detected when MO was present at higher proportions in PEG 4000 and in PEG 1500 but not in PEG 8000. Thus, we hypothesize that one phase was already present shortly after solidification, and that the other formed as more MO was expelled from the PEG-rich phase upon secondary crystallization of PEG molecules. The absence of the latter form in the PEG 8000 mixture was, according to the hypothesis, due to a low MO content in the initial PEG-rich phase, accompanied by a lower propensity for this molecular weight to unfold during secondary crystallization. Consequently, the amount of MO expelled from the PEG 8000 structure was below the detection limit of the methods used. This study shows how the molecular weight of PEG affects how MO is dispersed in a solid mixture of the two components. The different crystallization patterns of the PEGs determine the MO phase formation but the crystallization of PEG is also affected by the presence of MO. This knowledge is useful in further studies on fundamentals of phase formation in solid polymer materials, as well as when solid dispersions are to be developed as drug carrier systems.

Acknowledgements

Danisco Cultor is gratefully acknowledged for the MO. J.U. and S.E. acknowledge the support from Chalmers Foundation.

References

- [1] Humberstone AJ, Charman WN. *Adv Drug Delivery Rev* 1997;25(1): 103–28.
- [2] Mercke Odeberg J, Kaufmann P, Kroon KG, Hoglund P. *Eur J Pharm Sci* 2003;20(4–5):375–82.
- [3] Garcia-Fuentes M, Torres D, Alonso MJ. *Colloids Surf, B: Biointerfaces* 2003;27(2–3):159–68.
- [4] Pouton CW. *Eur J Pharm Sci* 2000;11:S93–S8.
- [5] Zimmermann E, Müller RH. *Eur J Pharm Biopharm* 2001;52(2):203–10.

- [6] Pedersen GP, Fäldt P, Bergenståhl B, Kristensen HG. *Int J Pharm* 1998; 171(2):257–70.
- [7] Meinzer A, Mueller E, Vonderscher J. *Journées Galéniques* 1995;8821–6.
- [8] Corveleyn S, Remon JP. *Int J Pharm* 1998;166(1):65–74.
- [9] Mehnert W, Mader K. *Adv Drug Delivery Rev* 2001;47(2–3):165.
- [10] Spicer PT, Small WB, Lynch ML, Burns JL. *J Nanopart Res* 2002;4(4): 297–311.
- [11] Mahlin D, Ridell A, Frenning G, Engström S. *Macromolecules* 2004; 37(7):2665–7.
- [12] Mahlin D, Ridell A, Frenning G, Engström S. *Macromolecules* 2004; 37(10):3958.
- [13] Engström S. *Lipid Technol* 1990;242–5.
- [14] Norling T, Lading P, Engström S, Larsson K, Krog N, Nissen SS. *J Clin Periodontol* 1992;19(9):687–92.
- [15] Shah JC, Sadhale Y, Chilukuri DM. *Adv Drug Delivery Rev* 2001; 47(2–3):229–50.
- [16] Landau EM, Rosenbusch JP. *Proc Natl Acad Sci USA* 1996;93(25): 14532–5.
- [17] Buckley CP, Kovacs AJ. *Colloid Polym Sci* 1976;254(8):695–715.
- [18] Sjökvist E, Nyström C, Aldén M. *Int J Pharm* 1989;54(2):161–70.
- [19] Wulff M, Aldén M. *Thermochim Acta* 1995;256(1):151–65.
- [20] Wulff M, Aldén M, Craig DQM. *Int J Pharm* 1996;142(2):189–98.
- [21] Morris KR, Knipp GT, Serajuddin ATM. *J Pharm Sci* 1992;81(12): 1185–8.
- [22] Pielichowski K, Flejtuch K. *Macromol Mater Eng* 2003;288(3):259–64.
- [23] Stribeck N, Alamo RG, Mandelkern L, Zachmann HG. *Macromolecules* 1995;28(14):5029–36.
- [24] Huang CI, Chen JR. *J Polym Sci, Part B: Polym Phys* 2001;39(21): 2705–15.
- [25] Dreezen G, Koch MHJ, Reynaers H, Groeninckx G. *Polymer* 1999; 40(23):6451–63.
- [26] Shieh YT, Lin YG, Chen HL. *Polymer* 2002;43(13):3691–8.
- [27] Toraya H. *J Appl Crystallogr* 1986;19440–7.
- [28] Craig DQM. *Drug Dev Ind Pharm* 1990;16(17):2501–26.
- [29] Santa Cruz C, Stribeck N, Zachmann HG, Baltá Calleja FJ. *Macromol-ecules* 1991;24(22):5980–90.
- [30] Malkin T. *Prog Chem Fats Lipids* 1954;21–50.
- [31] Yeh F, Hsiao BS, Chu B, Sauer BB, Flexman EA. *J Polym Sci, Part B: Polym Phys* 1999;37(21):3115–22.
- [32] Young RJ, Lovell PA. *Phase-separation behaviour of polymer solutions. Introduction to polymers*. London: Chapman and Hall; 1991 p. 203–212.